Available online at www.sciencedirect.com

SciVerse ScienceDirect

Ceramics International 38 (2012) 3513–3518

CERAMICS INTERNATIONAL

www.elsevier.com/locate/ceramint

Short communication

Al_2O_3–MgO castables performance in an expansion constrained environment

E.Y. Sako *, M.A.L. Braulio, V.C. Pandolfelli

Federal University of São Carlos – Materials Microstructural Engineering Group (FIRE Associate Laboratory), Rod. Washington Luiz, km 235, C.P. 676, CEP 13565-905, São Carlos, Brazil

Received 8 December 2011; received in revised form 15 December 2011; accepted 16 December 2011
Available online 27 December 2011

Abstract

The present work addresses the importance of considering the working structural conditions when evaluating the expansive behavior of alumina–magnesia castables under chemical corrosion. Slag resistance tests were conducted on spinel castables with different expansion levels, inserted in cement-bonded high alumina blocks, to limit their expansion, and compared to the results attained after performing the same experiments without any constraint. The results pointed out that in an expansion controlled condition, the penetration indexes were reduced as a result of the lower volume of pores in the castable microstructure. Moreover, this benefit was enhanced for the coarser MgO-containing materials, contradicting the trends usually observed when no structural constraint is considered.

Keywords: C. Corrosion; D. Spinel; Expansion under constraint

1. Introduction

Among the most relevant oxides added to refractories for steelmaking applications, magnesium aluminate spinel ($MgAl_2O_4$) stands out for both, its chemical stability and the positive volume change associated with its *in situ* formation reaction [1]. If, on one hand, this expansion may close joints and generate compressive stresses [2], on the other it may also decrease the refractory performance when it is poorly designed [3]. In this context, great efforts have been placed in order to produce spinel-forming castables with a designed permanent expansion, taking into consideration the grain size of the reactants, the binder source and even the aggregates' composition [4–7].

However, most of the studies related to this subject are usually conducted in expansion-free environments, whereas service structural conditions involve limited allowance for volumetric change [8]. In the latter case, a restrained expansion could act as a strengthening mechanism by partially filling the castable porosity. Therefore, the best results attained in the laboratory could not be the same in practice.

A suitable example is the corrosion resistance evaluation of the steel ladle refractory lining, which is constantly exposed to the aggressive chemical attack of the basic slag from the refining process. Due to its direct relationship with the castable porosity and average pore size [9], besides the chemical aspects, the material's corrosion level depends on whether the castable is surrounded by a physical barrier or not.

By using electrofused alumina-based crucibles to refrain the castable expansion, Soudier et al. [10] attempted to evaluate the corrosion resistance of spinel castables with different expansive behavior in two testing conditions: partially constrained or free to expand. Nonetheless, as the authors changed the castables' composition in order to attain different overall volume change, no clear correlation between the expansion level and corrosion degree in both environments could be observed. Therefore, the structural conditions played a less important role than the different chemical interactions between refractory and slag during testing.

In order to overcome this issue and present an additional method to evaluate the effects of a constrained environment on the refractory properties, in the present work castables with the same composition, but different expansion levels, were used.

* Corresponding author.
E-mail addresses: eric.ysako@gmail.com, vicpando@ufscar.br (E.Y. Sako).

0272-8842/$36.00
doi:10.1016/j.ceramint.2011.12.039

Table 1
Formulations of the evaluated alumina–magnesia castables (content of the raw materials in wt%).

Raw materials	Content, wt%		
	AM13	AM45	AM100
Tabular alumina ($D \leq 6$ mm)	80	80	80
Reactive alumina ($D \leq 4$ μm)	7	7	7
Dead-burnt MgO			
($D \leq 13$ μm)	6	–	–
($D \leq 45$ μm)	–	6	–
($D \leq 100$ μm)	–	–	6
CAC	6	6	6
Microsilica	1	1	1

2. Experimental procedures

Three alumina–magnesia castables (AM13, AM45 and AM100) designed by Braulio et al. [5,11] were selected to evaluate the effects of a structural constrained environment during the material's sintering. As shown in Table 1, tabular alumina (T-60, $D \leq 6$ mm, Almatis, Germany) was chosen as coarse aggregates and, for the *in situ* spinel reaction, reactive alumina (CL370, Almatis, Germany) and dead-burnt magnesia (95 wt% of MgO, CaO/SiO_2 ratio = 0.37 Magnesita Refratários S.A., Brazil) were added to the castable matrix. The compositions also comprised 6 wt% of calcium aluminate cement (Secar 71, 70 wt% of Al_2O_3, Kerneos, USA) as the binder and 1 wt% of microsilica (971 U, Elkem, Norway). The only difference in the castables' formulations was the magnesia grain size ($D_{max} \leq 13$, ≤45 and ≤100 μm), which ensured different expansion levels without changing the castable chemical composition.

After mixing the dry castables' powders and the required water content, prismatic samples (150 mm × 25 mm × 25 mm) were prepared under vibration, cured for 24 h at 50 °C in a humid environment (100% of relative humidity), dried for 24 h at 110 °C and calcined at 600 °C (1 °C/min) for 5 h in order to withdraw all the chemically bonded water. The samples were then fired at 1500 °C for 5 h in two different structural conditions: expansion free and under constraint.

A cement-bonded (6 wt% of CAC) high alumina castable with excellent mechanical strength ($\sigma_f > 50$ MPa – 3pt bending test) was produced and cast around the alumina–magnesia samples in order to impose the desired constraint, according to the sketch presented in Fig. 1.

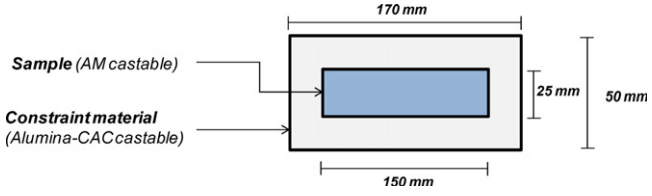

Fig. 1. Methodology used to apply a structural constraint during the firing of alumina–magnesia castables.

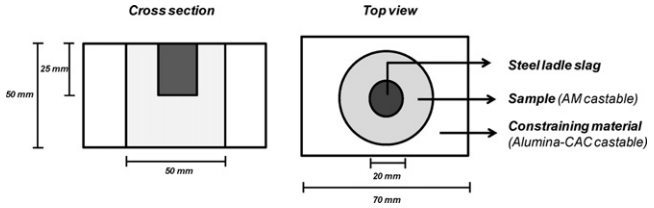

Fig. 2. Schematic assemblage of the sample used to perform the slag resistance experiments under structural constraint conditions.

After firing at 1500 °C for 5 h, the sample was withdrawn from its surrounding material and the following properties were measured.

Permanent linear expansion (PLE): Measured by the percentual difference between the initial and the final length (before and after heat treatment) divided by the initial sample dimension.

Apparent porosity and apparent density: Evaluated by using the Archimedes technique in kerosene, following the ASTM Standard C380.

Volume of pores: Scanning electron microscopy (SEM) images of the castables microstructure after firing at 1500 °C were attained (JEOL JSM – 5900 IV, the Netherlands). Based on these images, the volume of pores in the castable matrix was estimated using image analyzer software (Image J 1.42q, Wayne Rasband, National Institutes of Health, USA).

The same measurements were conducted for the castables fired at 1500 °C for 5 h without any constraint in order to compare the effects of expansion free conditions with those of the constrained ones.

For the corrosion resistance tests, the structural constraint was imposed using the same high-mechanical strength castable used to inhibit the expansion of the prismatic samples. For this evaluation, the alumina–CAC castable was firstly shaped as stated in Fig. 2 and after its curing (50 °C/24 h), drying (110 °C/24 h) and sintering (1500 °C/5 h) steps, the alumina–magnesia castable was moulded inside its inner hole. After pre-firing the assemblage (sample + constrained material) at 600 °C/5 h, the corrosion experiment was carried out for 5 h at 1500 °C using 10 g of a high-FeO_x steel ladle slag (Table 2). The same testing conditions were applied for the non-constrained castables.

After testing, the corroded samples were cut and the penetration indexes were calculated in order to measure the corrosion damage using the Image J 1.42q software (Wayne Rasband, National Institutes of Health, USA), according to the procedure described by Braulio et al. [12].

3. Results and discussion

Fig. 3a presents the samples' cross-sections (AM13, AM45 and AM100) after the corrosion experiments were

Table 2
Chemical composition of the steel ladle slag used in the corrosion experiments.

Composition (wt%)	MgO	Al_2O_3	SiO_2	CaO	MnO	FeO_x
	8.8	1.7	7.5	34.2	3.6	43.6

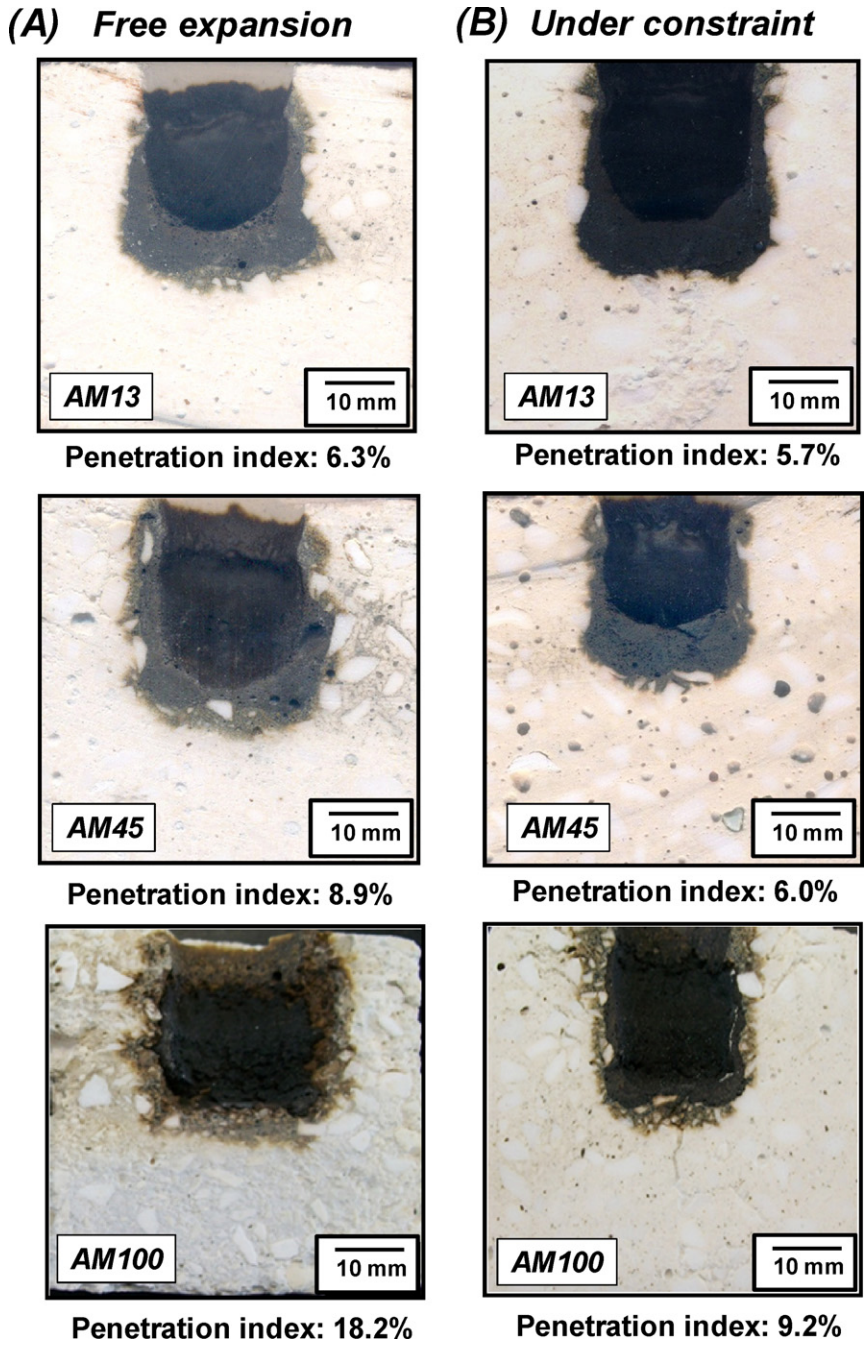

Fig. 3. Samples' cross sections of the AM13, AM45 and AM100 castables and their penetration indexes after the corrosion experiments (a) in an expansion free environment or (b) under constraint.

conducted in an expansion free condition and their respective penetration indexes. In this case, the infiltration degree scaled with the average magnesia grain size, leading to an inferior performance of AM100 castable. According to Sako et al. [13], the corrosion mechanisms of spinel castables are ruled by the CA_6 phase distribution in the microstructure before the slag attack. When nucleated at the tabular alumina aggregates, the calcium hexaluminate crystals react with the slag leading to a solid and dense CA_2 layer, which protects the aggregates and inhibits further infiltrations. Conversely, when CA_6 formation takes place mainly in the matrix, the unprotected aggregates are quickly consumed by the slag, resulting in additional CA_6 grains as a product of the refractory-liquid interaction. In this latter case, cracks are also formed due to the hexaluminate expansive feature, inducing the liquid infiltration and spoiling the castable performance.

Fig. 4 shows the microstructure of the evaluated samples after pre-firing at 1500 °C for 5 h. It can be observed that CA_6 crystals followed the same distribution pattern in all of them: mostly at the edges of tabular alumina aggregates, with a minor presence in the matrix. Therefore, the chemical corrosion mechanism should in principle be the same, regardless of the MgO grain size.

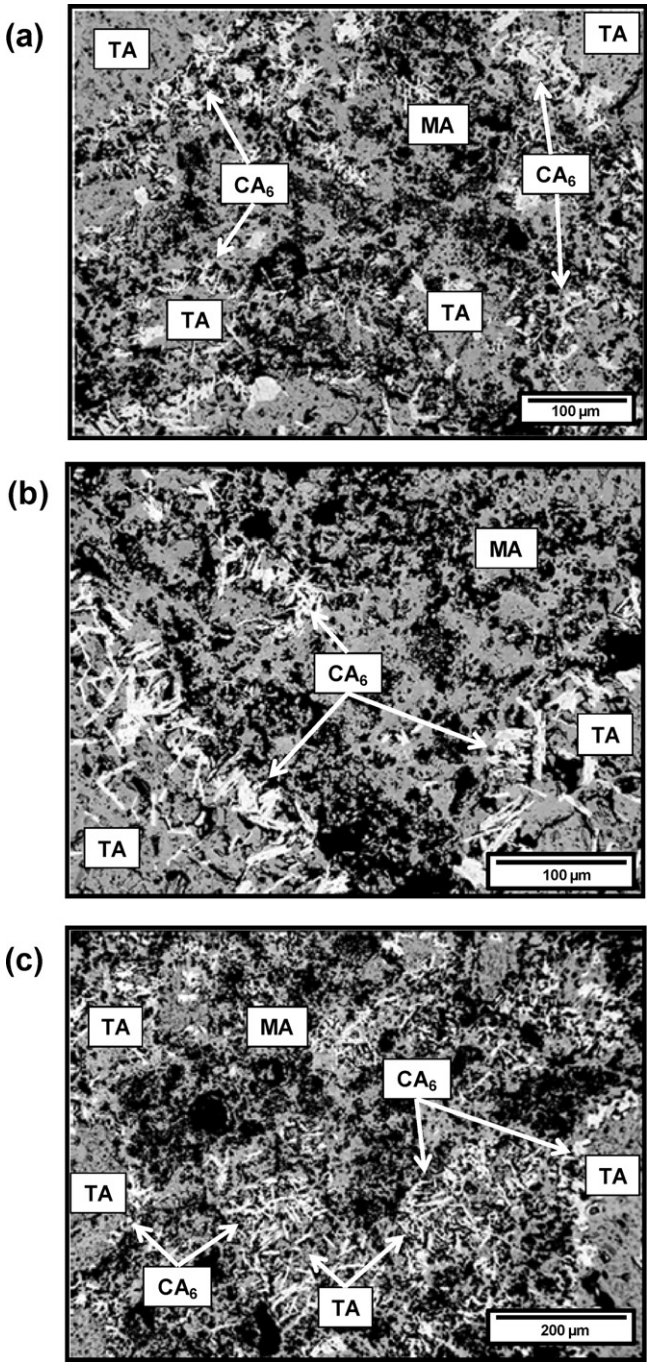

Fig. 4. Microstructural profile of the castables AM13, AM45 and AM100 after firing at 1500 °C/5 h, highlighting the CA_6 crystals distribution in the microstructure.

However, although presenting the same microstructural profile, Sako et al. [14] stated that some physical properties of castables containing MgO with different granulometry differed significantly when fired without any constraint. According to these authors, the one-direction flux of Mg^{2+} ions for the spinel reaction and the Kirkendall effect led to pore formation where the magnesia particles were originally placed. As a consequence, the microstructure of the castable containing coarser MgO (AM100) presented a higher number of large pores.

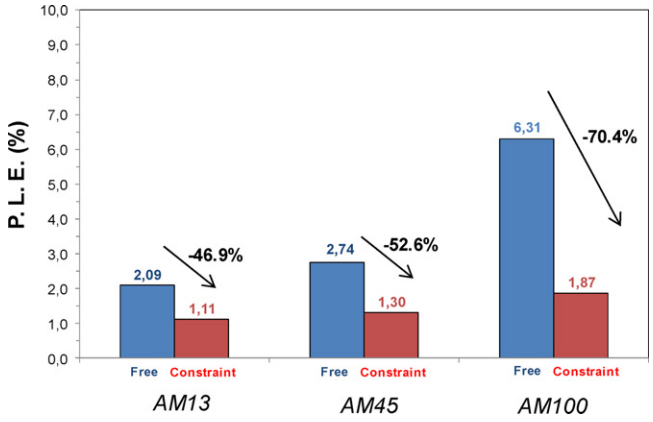

Fig. 5. (a) Permanent linear expansion (P.L.E.) of the alumina–magnesia castables containing different MgO grain sizes after firing at 1500 °C/5 h under constraint and in expansion free environments.

In addition, when free to expand, the permanent linear change (Fig. 5) and the apparent porosity (Fig. 6a) values scaled with the increase in the magnesia grain size, which, as a consequence, was followed by lower density (Fig. 6b). These results confirmed the higher expansion associated with the use of coarse MgO grains and its impact in the material's properties, which has already been stated by Braulio et al. [5]. The unfavorable association of such physical properties (large pores with high porosity) after firing at 1500 °C resulted

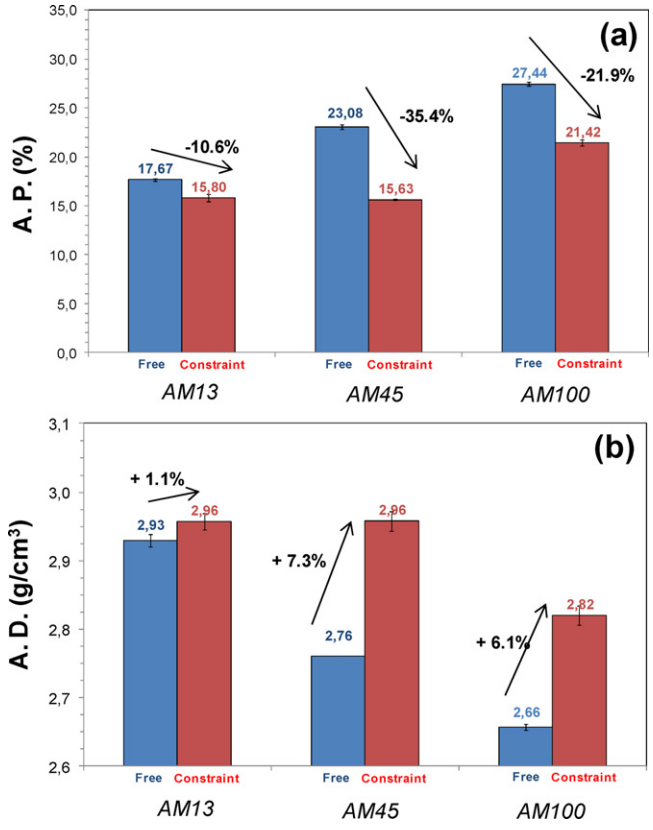

Fig. 6. (a) Apparent porosity (A.P.) and (b) apparent density (A.D.) of the alumina–magnesia castables containing different MgO grain sizes after firing at 1500 °C/5 h under constraint and in expansion free environments.

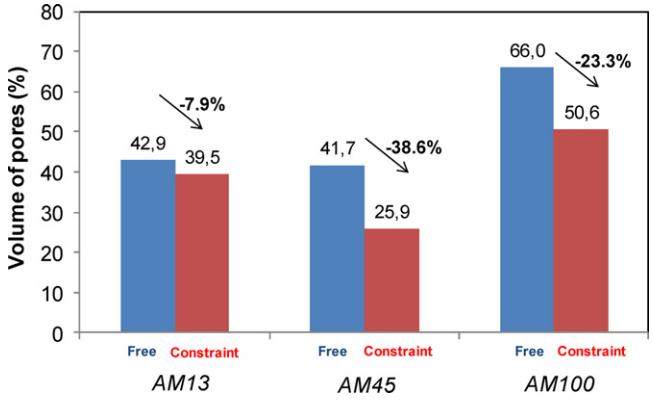

Fig. 7. Volume of pores in the matrix of the castables AM13, AM45 and AM100 after firing at 1500 °C/5 h in expansion free or constrained structural conditions, estimated from SEM images in Fig. 4.

in the deeper slag penetration observed in Fig. 3a for the AM100 sample.

The physical barrier imposed to simulate service structural conditions during firing seemed to play an efficient role on the castables' performance. In Fig. 3b, one can notice the benefits on the reduction in the slag penetration index which scaled with the MgO grain size. In fact, the result attained for the AM100 sample under constraint was close to the ones for the compositions with lower P.L.E., but with no physical barrier. This improvement is a consequence of the expansion constraint observed in Fig. 5, as for these samples, the volumetric expansion was forced to fill in the castables intrinsic porosity, resulting in a higher densification. The results in Fig. 6 clearly show that this benefit is enhanced for the coarser MgO-containing materials.

Thus, a restrained expansion helped to reduce the available paths for the slag physical infiltration, which is confirmed in Fig. 7. Based on SEM images, it presents the estimated volume of pores in the matrix of each castable after heat treatment, confirming the densifying effect imposed by the alumina–CAC barrier.

All these results highlighted the main reasons for selecting *in situ* spinel-forming castables to produce high-performance pre-shaped components for steelmaking units. As previously stated by the authors [13], even presenting an expansive behavior and higher porosity, the corrosion resistance of this sort of castable is higher when compared to pre-formed spinel-containing ones, due to the suitable microstructural configuration. When considering the working conditions, this superiority is even more evident, as the *in situ* spinel intrinsic volumetric change can be faced as a positive effect in the actual constrained steel vessels environment.

Moreover, the enhanced performance of AM100 composition under constraint pointed out a relevant opportunity for using coarse magnesia grains in order to reduce the castable hydration trend and, consequently, the processing drawbacks, such as crack formation during drying. Nevertheless, one must take into account that none of the above-mentioned benefits will be fulfilled in practice if the surrounding refractories do not withstand the stress generated by the restrained expansion. In this case, they will crack and release the pre-shaped component from its constrained condition.

4. Conclusions

The results obtained in this work pointed out that, in service, alumina–magnesia castables can present a higher performance than the ones usually attained in laboratory conditions, as a consequence of the constrained environment. When free to expand, castables containing coarser MgO grains usually present poor corrosion behavior, owing to the higher residual expansion, which helps the physical slag infiltration. Nonetheless, in an expansion controlled condition, the penetration indexes were reduced as a result of the lower volume of pores and flaws closure in the castable microstructure.

Unlike what is reported in the literature, the results showed that, when only the castable expansion level was considered and its chemical and mineralogical composition was kept constant, the structural constraint played a relevant role in some important properties. The results indicated that a suitable experimental design can be as significant as the material's microstructural one to predict the lining performance in the steelmaking operations.

Acknowledgments

The authors are grateful to the Federation for International Refractories Research and Education (FIRE) and the Brazilian funding agency CNPq for supporting this work; and Leandro H. Costa, for conducting the slag resistance experiments.

References

[1] S. Zhang, W.E. Lee, Spinel-containing refractories, in: S. Zhang, W.E. Lee (Eds.), RefractoriesHandbook, Marcel Dekker Inc., USA, 2004, pp. 215–257.
[2] S. Chen, M. Cheng, S. Lin, Y. Ko, Thermal characteristics of Al_2O_3-spinel castables for steel ladles, Ceramics International 28 (2002) 811–817.
[3] M.A.L. Braulio, M. Rigaud, A. Buhr, C. Parr, V.C. Pandolfelli, Spinel-containing alumina-based refractory castables, Ceramics International 37 (6) (2011) 1705–1724.
[4] M.A.L. Braulio, M.F. Piva, G.F.L. Silva, V.C. Pandolfelli, In situ spinel expansion designed by colloidal alumina suspension addition, Journal of American Ceramic Society 92 (2) (2009) 559–562.
[5] M.A.L. Braulio, L.R.M. Bittencourt, V.C. Pandolfelli, Magnesia grain size effect on *in situ* spinel refractory castables, Journal of European Ceramic Society 28 (2008) 2845–2852.
[6] M.A.L. Braulio, D.H. Milanez, E.Y. Sako, L.R.M. Bittencourt, V.C. Pandolfelli, Expansion behavior of cement-bonded alumina–magnesia refractory castables, American Ceramic Society Bulletin 86 (12) (2007) 9201–9206.
[7] M.A.L. Braulio, D.H. Milanez, E.Y. Sako, L.R.M. Bittencourt, V.C. Pandolfelli, Are refractory aggregates inert? American Ceramic Society Bulletin 87 (3) (2008) 27–32.
[8] J. Mori, N. Watanabe, M. Yoshimura, Y. Oguchi, T. Kwakami, Material design of monolithic refractories for steel ladle, American Ceramic Society Bulletin 69 (7) (1990) 1172–1176.
[9] W.R. Lee, S. Zhang, Melt corrosion of oxides and oxide-carbon refractories, International Materials Reviews 44 (3) (1999) 77–104.
[10] J. Soudier, P. Meunier, V. Nozahic, Characterisation of alumina–magnesia castables after firing in expansion controlled environment, in: Proceedings of UNITECR 2009, Salvador, Brazil, (2009), pp. 59–63.

[11] M.A.L. Braulio, J.F. Castro, C. Pagliosa, L.R.M. Bittencourt, V.C. Pandolfelli, From macro to nanomagnesia: designing the *in situ* spinel formation, Journal of the American Ceramic Society 91 (9) (2008) 3090–3093.

[12] M.A.L. Braulio, A.P. Luz, A.G. Tomba Martinez, C. Liebske, V.C. Pandolfelli, Basic slag attack of spinel-containing refractory castables, Ceramics International (2011), doi:10.1016/j.ceramint.2011.02.007.

[13] E.Y. Sako, M.A.L. Braulio, V.C. Pandolfelli, The corrosion and microstructure relationship for cement-bonded refractory castables, Ceramics International (2011), doi:10.1016/j.ceramint.2011.10.061.

[14] E.Y. Sako, M.A.L. Braulio, E. Zinngrebe, S.R. van der Laan, V.C. Pandolfelli, Fundamentals and applications on in situ spinel formation mechanism in Al_2O_3–MgO refractory castables, Ceramics International (2011), doi:10.1016/j.ceramint.2011.10.074.